All-Optical Label Swapping Networks and Technologies

Daniel J. Blumenthal, *Senior Member, IEEE, Member, OSA*, Bengt-Erik Olsson, Giammarco Rossi,
Timothy E. Dimmick, Lavanya Rau, Milan Mašanović, Olga Lavrova, *Student Member, IEEE*, Roopesh Doshi,
Olivier Jerphagnon, John E. Bowers, *Fellow, IEEE*, Volkan Kaman, Larry A. Coldren, *Fellow, IEEE, Fellow, OSA*,
and John Barton

Invited Paper

Abstract—**All-optical label swapping is a promising approach to ultra-high packet-rate routing and forwarding directly in the optical layer. In this paper, we review results of the DARPA Next Generation Internet program in all-optical label swapping at University of California at Santa Barbara (UCSB). We describe the overall network approach to encapsulate packets with optical labels and process forwarding and routing functions independent of packet bit rate and format. Various approaches to label coding using serial and subcarrier multiplexing addressing and the associated techniques for label erasure and rewriting, packet regeneration and packet-rate wavelength conversion are reviewed. These functions have been implemented using both fiber and semiconductor-based technologies and the ongoing effort at UCSB to integrate these functions is reported. We described experimental results for various components and label swapping functions and demonstration of 40 Gb/s optical label swapping. The advantages and disadvantages of using the various coding techniques and implementation technologies are discussed.**

I. INTRODUCTION

INTERNET traffic is growing exponentially and is forcing next generation Internet Protocol (IP) networks to scale far beyond present speed, capacity, performance, and packet forwarding rates. In fiber-based optical networks, next generation optical IP routing will require technologies to support packet routing and forwarding operations at Terabit wire rates that are compatible with wavelength division multiplexed (WDM) transmission and routing. Up to 50% of IP traffic consists of packets smaller than 522 bytes and 50% of these packets are in the 40–44 byte range. New low-latency packet forwarding and routing technologies will be required that can handle wire-rate routing of the smallest packets at rates in excess of Gigapackets/s. These technologies should support new streamlined IP routing protocols such as Multiprotocol Label Swapping (MPLS) [1] that simplify route lookup and separate the routing and forwarding functions.

All-Optical Label Swapping (AOLS) [2]–[4] implements the packet-by-packet routing and forwarding functions of MPLS directly in the optical layer. This is in contrast to next generation commercial optical networks that will use MPLS to set up optical circuits over which flows of electronic packets are routed [5]. For future optical networks, it will be desirable to perform optical routing layer functions independent of the IP packet length and payload bit rate. AOLS approaches should interface seamlessly to both WDM and TDM systems. This leads to the concept of using optical labels to "encapsulate" the IP packet in the optical layer. The optical label format is chosen to best match the optical routing and forwarding technology and to satisfy other constraints in the optical layer (e.g., the current lack of flexible optical buffering technologies).

In this paper, we describe AOLS research at the University of California at Santa Barbara (UCSB) supported under the DARPA sponsored Next Generation Internet (NGI) program and the DARPA sponsored Center for Multidisciplinary Optical Switching Technology (MOST) and the NGI partner Cisco Systems and NGI industrial affiliates New Focus, Agilent Technologies, and Netcom Systems and performed in collaboration with the DARPA supported NGI program at Telecordia Technologies.

The paper is organized into seven sections. Section II describes the overall concept of AOLS, its application in optical networks and optical Internet protocol routers. The key building blocks used to implement AOLS are also described. In Section III we review two different label-coding techniques that
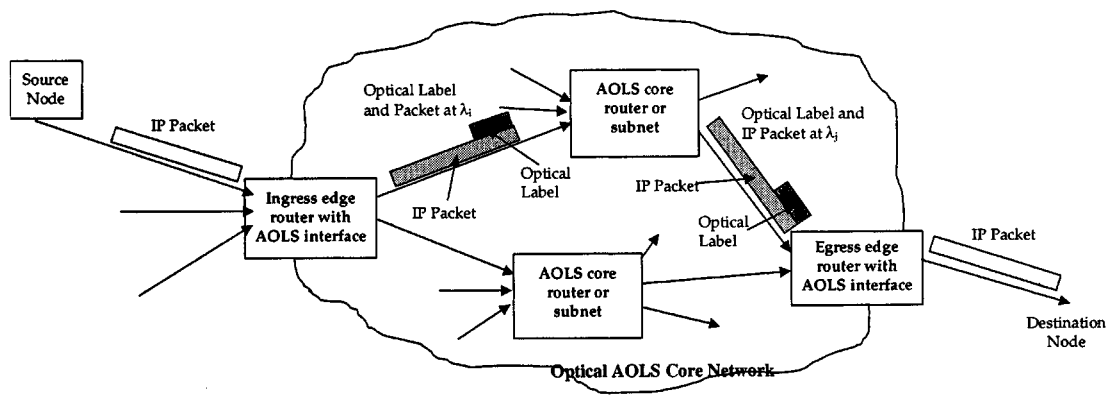
Fig. 1. Optical label swapping with wavelength conversion in an optical core network using edge and core WDM IP routers.
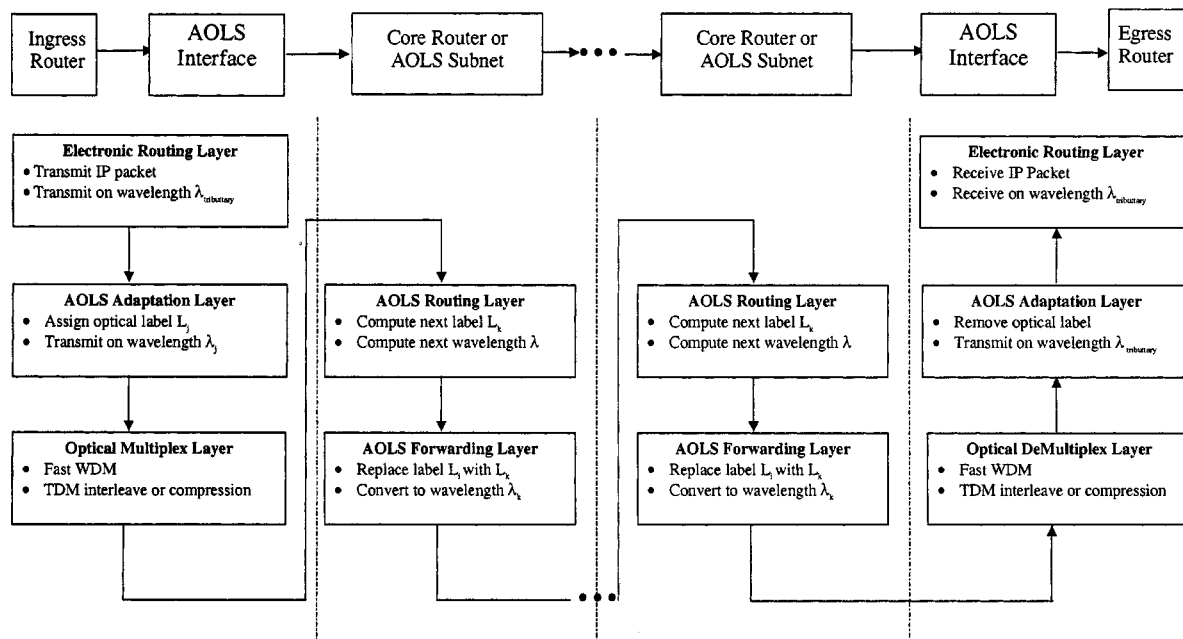

Fig. 2. Layered routing and forwarding hierarchy and associated network element connection diagram for an AOLS network.

have been used to date. Section IV introduces issues specific to building multihop AOLS networks. Several technologies that have been used to realize AOLS building blocks are covered in Section V and the AOLS subsystems are covered in Section VI. Systems experimentally demonstrated at UCSB are described in Section VII.

II. ALL-OPTICAL LABEL SWAPPING (AOLS)

An AOLS optical packet core network is illustrated in Fig. 1. IP packets enter the core network at an ingress router and travel multiple hops through the core, exiting at an egress router. Packets are handled within the network by core AOLS routers or AOLS subnets, as described in [2]. Fig. 2 depicts the physical network elements connected by fiber links and the packet routing and forwarding hierarchy. IP packets are generated at the electronic routing layer and processed in an adaptation layer that "encapsulates" IP packets with an optical label without modifying the original packet structure. The adaptation layer also shifts the packet and label to a new

wavelength specified by local routing tables. An optical multiplexing layer multiplexes labeled packets onto a shared fiber medium. Several optical multiplexing approaches may be used including insertion directly onto an available WDM channel, packet compression through optical time division multiplexing or time interleaving through optical time division multiplexing [6]. This technique is not limited to IP packets and other packet or cell structures like ATM may also be routed.

Once inside the core network, core routers or AOLS subnets [2] perform routing and forwarding functions. The routing function computes a new label and wavelength from an internal routing table given the current label, current wavelength, and fiber port. The routing tables (at egress and core routers) are generated by converting IP addresses into smaller pairs of labels and wavelengths and distributing them across the network much in the same way that multiprotocol label switching (MPLS) is used in today's IP networks [1]. The forwarding function involves swapping the original label with the new label and physically converting the labeled packet to the new wavelength. Other switching or buffering mechanisms (space, time, etc.) are also
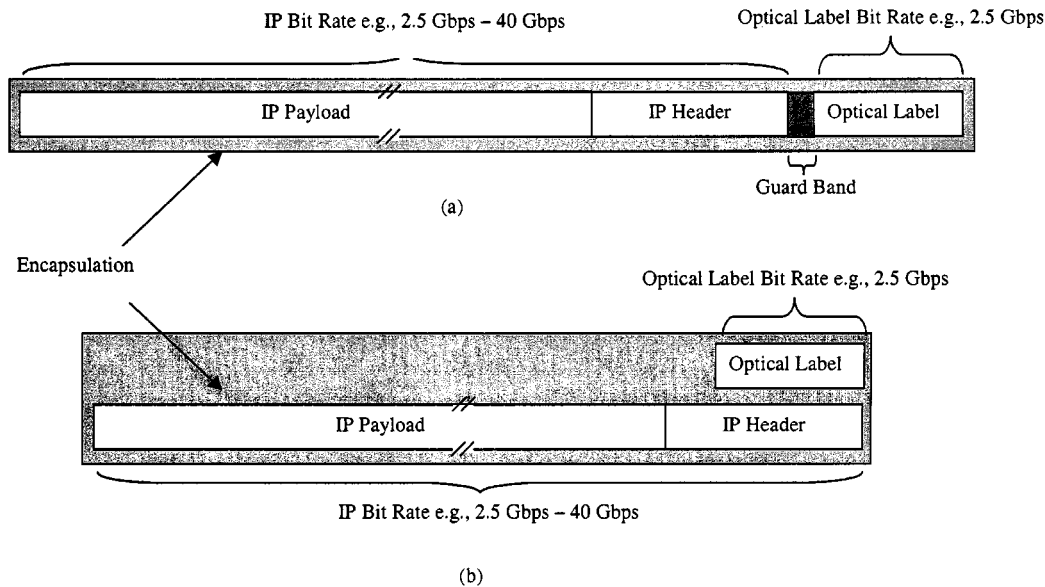
Fig. 3.   Optical label coding techniques: (a) fixed rate serial label and (b) optical subcarrier multiplexed label.

configured in the forwarding process. The reverse process of optical demultiplexing, adaptation and electronic routing are performed at the egress node.

III. OPTICAL LABEL CODING TECHNIQUES

The method of coding the label onto a packet impacts the channel bandwidth efficiency, the transmission quality of the packet and label, and the best method to wavelength convert the packet and optically swap the label. Two approaches to optical label coding are the serial label [7], [8] and the optical subcarrier multiplexed label [3], [9]–[11], as illustrated in Fig. 3. With serial coding a fixed bit rate label is multiplexed at the head of the IP packet with the two separated by an optical guard-band (OGB) as shown in Fig. 3(a). The OGB is use to facilitate label removal and reinsertion without static packet buffering and to accommodate finite switching times of optical switching and wavelength conversion. The bit-serial label is encoded on the same optical wavelength as the IP packet and is encoded as a baseband signal. For optical subcarrier multiplexed labels a baseband label is modulated onto a RF subcarrier and then multiplexed with the IP packet on the same wavelength [see Fig. 3(b)]. This multiplexing may be performed electronically or optically as described in [2]–[4], [12]–[14]. An OGB is not necessary in the subcarrier case since the label is transmitted in parallel with the packet. It is only necessary that the label fit within the boundaries of the packet, however an OGB may be used if accumulated misalignment of the label and payload occurs during multiple hops.

Packet transparency is realized by setting a fixed label bit rate and modulation format independent of the packet bit rate. The choice of label bit rate is driven by a combination of factors including the speed of the burst-mode label recovery electronics and the duration of the label relative to the shortest packets at the fastest packet bit rates. Additionally, running the label at a lower bit rate allows the use of lower cost electronics to process the

label. The label and packet bits can be encoded using different data formats to facilitate data and clock recovery. For example, if the IP packet is compressed to 40 Gb/s using an RZ data format, the label can be encoded at 2.5 Gb/s using NRZ format. A 20-bit label transmitted at 2.5 Gb/s occupies the same duration as a 40-byte packet transmitted at 40 Gb/s.

Encapsulation of IP packets using optical labels has advantages in that the contents of the original IP packet are not modified and the label is coded at the same wavelength as the IP packet. In the serial case, erasure and rewriting of the label may be performed independently of the IP packet bit rate, however, timing of the label replacement and possibly erasure process is somewhat time critical. The subcarrier labels have the advantage that they can be removed and replaced more asynchronously with respect to the packet but potentially suffer from dispersion induced fading, a problem that can be remedied as described in a later section.

IV. AOLS FUNCTIONS AND BUILDING BLOCKS

Label recovery, label swapping and packet forwarding are the basic functions handled by the AOLS building blocks, shown in Fig. 4. In a core router or AOLS subnet [see Fig. 4(a)], a burst-mode label recovery module is used to recover label clock and data for processing in electronic routing circuitry without significantly perturbing the through-going optical packet data. The routing circuit maps the incoming label and wavelength to a new label and wavelength based on internal routing tables. The label erasure process may be built into this stage depending on the implementation technology. The second stage performs label erasure (if not performed in the first stage), wavelength conversion and label rewriting using a wavelength converter or combination of converter and optical filter. A fiber optic delay follows the label recovery stage to match the routing processing delay with the arrival of the packet at the second optical stage. An edge router [see Fig. 4(a)] utilizes a slightly modified first
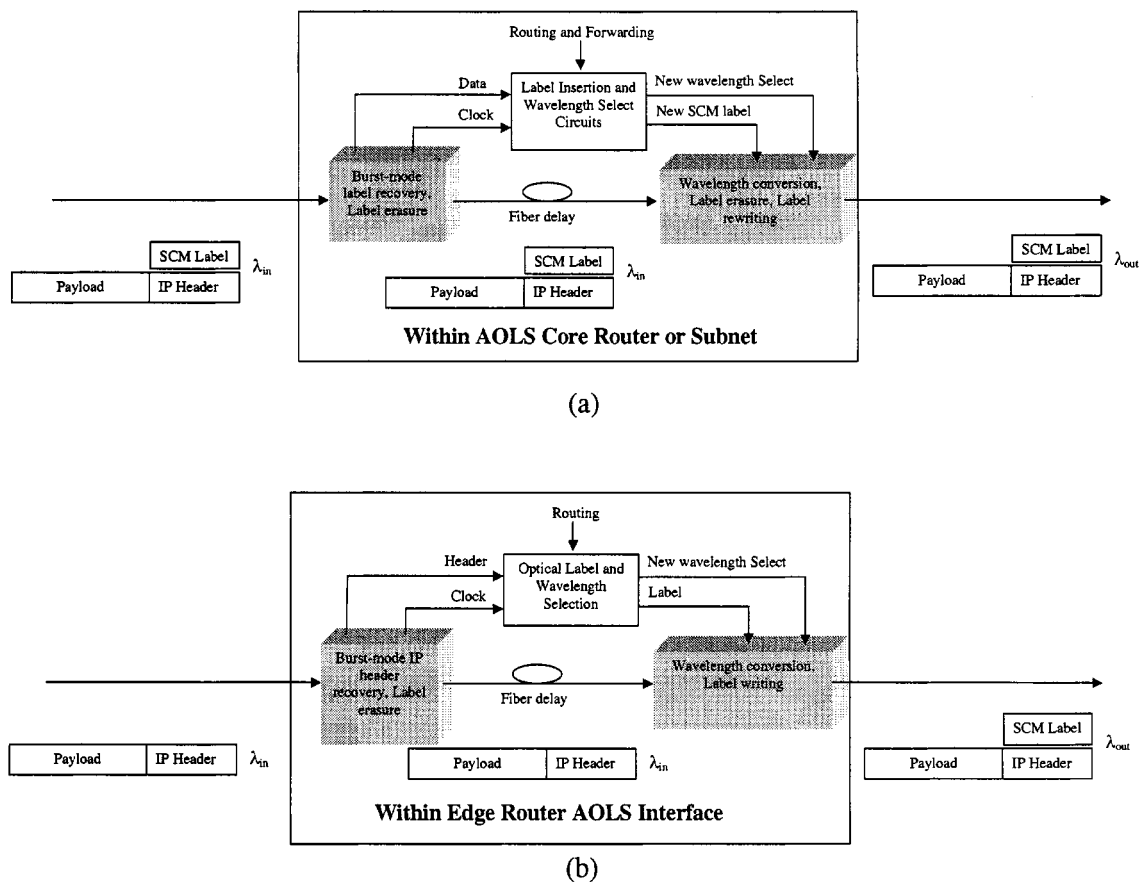
Fig. 4.   Building blocks for AOLS (a) core router and (b) core optical routers or subnets.

stage to detect the IP packet header with minimal disturbance to the packet. The second stage performs the same wavelength conversion and label rewriting processes as in the core router, however, the wavelength conversion may be optoelectronic-optic (OEO) depending on the network architecture.

V. ISSUES IN MULTIHOP AOLS NETWORKS

Routing in multihop optical packet network brings to the table a complex set of issues that must take into account the integrity of data transmission and the bursty nature of the data. We briefly discuss the three issues of routing in a burst-mode environment, cascadability, and buffering. Each issue is complex enough to dedicate a paper on the topic and many papers on packet congestion and buffering have been written to date [11], [15].

A. Burst Mode Routing

The main issues in burst-mode routing are summarized in Fig. 5. Packets arrive at a routing node with unknown amplitude and phase relative to a local time reference. The inter-packet spacing is also unknown. For subcarrier coded labels, the data envelope must be recovered from a detected subcarrier with unknown RF phase. For any coding technique, data and clock recovery must be performed without *a priori* knowledge of the optimal threshold or clock phase. To efficiently use the label channel, the header should be extracted within the first few bits. These qualities are addressed in burst-mode receiver technology described in several publications [16], [17]. The optical packet

channel must also be able to accommodate burst-mode operation. The process of label erasure, wavelength conversion, label rewriting, and potential packet regeneration must operate under similar conditions as the label receiver, particularly with respect to amplitude dynamic range.

B. Congestion and Buffering

Optical packet collisions can occur at any core router node or at the edge egress points. Additionally, congestion within the packet handling hardware can occur if the label routing and packet forwarding functions are not pipelined properly. The cumulative interface delay, which is defined as the time involved to route a packet from the input port to the output port of a router, is on the order of tens of micrometers in today's state-of-the-art routers. However with an optimally designed label-processing and routing unit, the time required to process a header should be less than 100 ns. In a bursty network, inter-packet time intervals are not constant, therefore, the incoming packets may have to be buffered while a packet is being routed. The improvement in the packet processing time reduces the buffering time and thereby decreases latency. The routing function should incorporate packet forwarding, label erasure and rewriting the new label. The new label must be replaced with minimum knowledge of the payload contents. Wavelength conversion can facilitate all the above functions. The subject of packet buffering and contention is not a focus of this paper, and there have been multiple publications on this subject [11], [15].
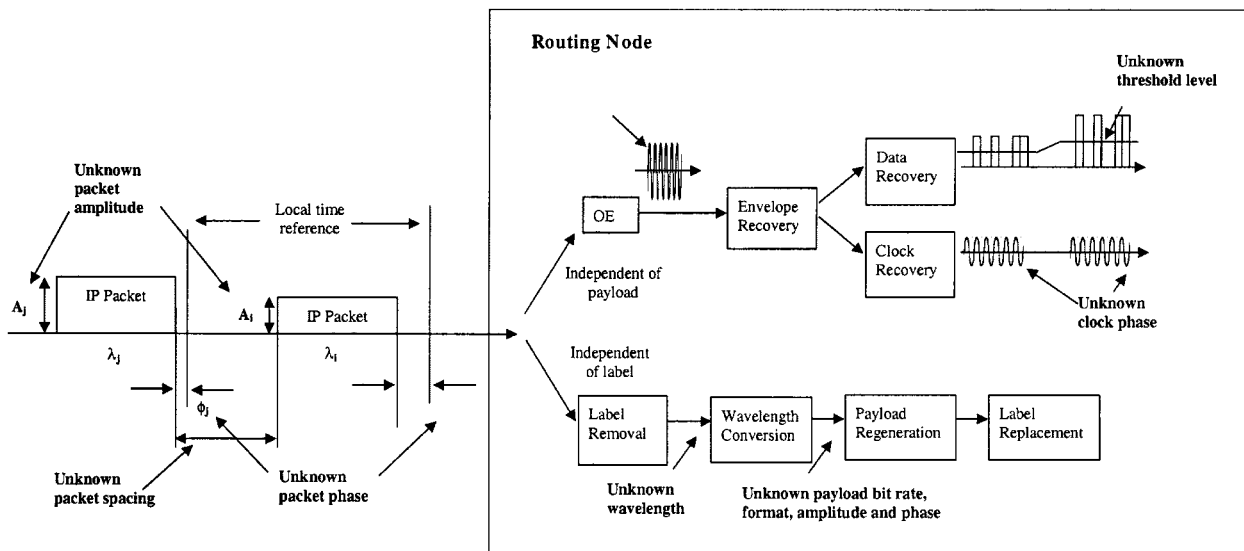
Fig. 5. At each router, label recovery/swapping and packet routing and forwarding must be performed on data that arrives on an unknown wavelength with unknown phase and amplitude.
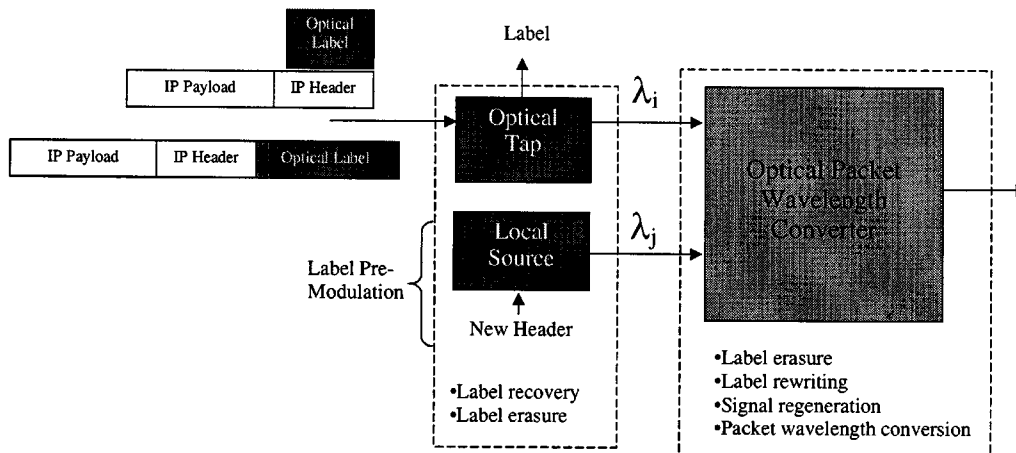

Fig. 6. General model of an AOLS wavelength converter subsystem.

VI. AOLS TECHNOLOGIES

In this section, we review various technologies that have been used to build AOLS subsystems and systems demonstrators. These technologies are classified into AOLS wavelength converters, fiber loop mirrors, wavelength agile sources, optical demultiplexers and packet transmitters.

A. AOLS Packet Wavelength Converters

In general, an AOLS packet wavelength converter performs the functions of label optical label erasure, packet rate wavelength conversion, packet regeneration and optical label rewriting. A general model of an AOLS wavelength converter subsystem including the label tap is shown in Fig. 6. Shown at the inputs of Fig. 6 are the two possible types of labeled packet inputs (serial or OSCM). Depending on the combination of label coding technique and wavelength converter technology, the label tap may or may not handle the label erasure function. A tap that handles the function of erasure and label recovery is described in the next section on fiber loop mirrors.

AOLS wavelength converters have the general capability to simultaneously erase and rewrite during the conversion process. If the label is placed in a properly designed region of the optical or electrical bandwidth or intensity, the packet data at (λ_i) is transferred over to the new wavelength (λ_j) and the label on the original wavelength is not transferred to (λ_j). At the same time, the new label may be pre-modulated onto the new wavelength source (λ_j) and will appear with the wavelength converted packet at (λ_j) and not be transferred to the original wavelength (λ_i). Certain wavelength converter geometries also allow the new header to be written into the wavelength converter module directly.

The packet wavelength converter is also used to perform signal regeneration of the packet to support multihop operation. This regeneration is at least 2R where the extinction ratio is enhanced and the "0" and "1" level noise reduced. 3R regeneration with retiming may also be performed [18].

1) Semiconductor Optical Amplifier (SOA) Based Converters: Cross-gain modulation (XGM) in SOAs is a well understood effect that allows an intensity-modulated signal to
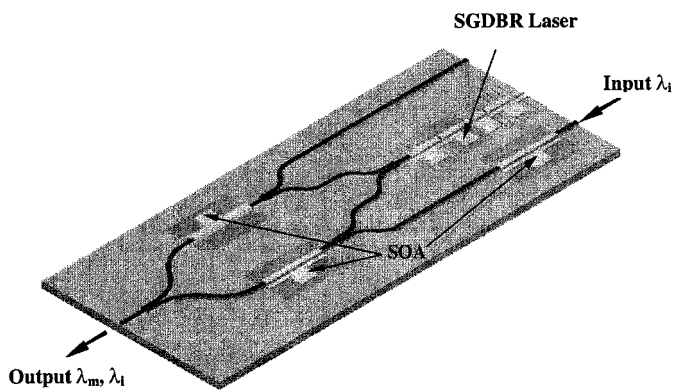
Fig. 7.   SOA-based MZI-WC layout of UCSB device.

be transferred from wavelength to another wavelength [19], [20]. Operation at 10 Gb/s or more is possible using this technique and polarization insensitive conversion is possible using amplifiers with polarization insensitive gain [21]. XGM technique decreases the extinction ratio of the output signal (8 dB) and is asymmetric for frequency-up-conversion and frequency-down-conversion. XGM can also introduce chirping and amplitude distortion unless designed properly. This conversion technique is bit rate transparent out to a maximum designed frequency and works for amplitude modulation schemes only. The XGM-WC is also an inverting converter and must be used in conjunction with a secondary device to provide noninverting operation that is important for multihop applications.

The cross phase modulation effect is utilized in an interferometer configuration and can be realized using SOA-based waveguide structures. Fig. 7 shows a Mach–Zehnder interferometer wavelength converter (MZI-WC) under fabrication at UCSB under the NGI program. The input signal passes through one of the interferometer arms and optically modulates the phase of that arm. The interferometric effect converts this phase modulation to an amplitude modulation as the probe signal traverses both arms. XPM produces a high extinction ratio for the converted signal (better than 15 dB) due to its highly nonlinear transfer characteristic. The device may be operated in an inverting or noninverting mode, however, the threshold characteristic of the XPM-WC restricts the dynamic range of the input signal such that the average signal level rests at the proper transfer characteristic operating point. Due to its high quality output signal, this technique represents an attractive solution for AOLS systems. In a later section on AOLS implementations we describe how to combine XGM and XPM converters to gain the full functionality of and AOLS-WC. The signal integrity can be compromised by accumulated distortion of the payload and label due to fiber dispersion and nonlinearities and accumulated SNR degradation due optical amplifier noise and system nonlinearities [3], [4]. Dispersion induced bit broadening, and, in particular, PMD [22], is a very important factor in high-speed (40 Gb/s and higher bit rate) systems. In general, the SNR and bit shape of packets with bit rate of 10 Gb/s and greater will have to be managed or regenerated in multihop systems. Using 2R regeneration during the wavelength conversion process can address the dispersion-induced bit broadening and SNR degradation issues.

2) Fiber XPM Wavelength Converter: To allow operation at ultrahigh bit rates we have demonstrated a new wavelength converter based on nonlinearities in an optical fiber [23] that supports operation at 40 Gb/s and beyond (possibly up to several hundered gigabits per second). In this scheme, we utilize XPM in a dispersion shifted fiber imposed from the incoming data onto CW light, followed by conversion of the phase modulation to amplitude modulation using optical filtering, as shown in Fig. 8. The incoming data is combined with a CW light signal and sent through an optical fiber where the data imposes a phase modulation onto the CW light via fiber XPM. This phase modulation generates optical sidebands on the CW signal, which are converted to amplitude modulation by suppressing the original CW carrier using an optical notch filter. A conventional band-pass filter to select one of the two sidebands then follows the notch filter. However, in principle it is sufficient to use a single band pass filter, e.g., a fiber bragg-grating or fiber-loop mirror, provided that it can suppress the original CW carrier enough.

Fig. 9 shows the eye-pattern (a) before and (b) after wavelength conversion of 40 Gb/s data. The polarization dependence for XPM in a fiber is 5 dB and the polarization dependence as measured with a power meter for the wavelength converter could vary between 2 and 8 dB, depending on the position and bandwidth of the band-pass filter. However, the polarization dependence can be eliminated by utilizing polarization scrambling [24] or circularly polarized fiber [25]. Even though a long fiber was used, no stability problems were observed and the system was only mechanically polarization sensitive before combining the data and CW light. Since the filter arrangement was polarization insensitive environmental disturbances to the DSF did not affect the performance apart from a small timing shift, which can be compensated for by a clock recovery circuit.

Since this scheme relays on optical filtering the issue of wavelength tunability of the filters is critical. The wavelength converter must have the ability to be reconfigured to convert to an arbitrary wavelength within a few nanoseconds. Tunable lasers are today available that can be tuned to an arbitrary wavelength within less than a nanosecond [26] but tunable filters are usually not very fast. In a practical implementation, an important feature of a wavelength converter is to allow no conversion and conversion to wavelength channels near the input wavelength. Using this type of wavelength converter scheme, this can be achieved by simply switching the CW laser off and move the output filter to the actual wavelength and filter out a part of the due to self-phase modulation broadened spectrum [27]. Another important issue is cascadability of multiple wavelength converters. Due to the inherent nonlinear transmission and virtually instantaneous response of the wavelength converter it should be well suited for multi-hop operation. Simulations show that more than 100 hops can be passed without any significant degradation in SNR or timing jitter. This is, however, subject to further experimental investigations.

B. Suppressed Carrier SCM Taps Using Fiber Loop Mirrors (FLMs)

If double sideband SCM modulation is used to encode labels, periodic signal fading occurs due to fiber dispersion. The amount of fading will vary depending on the inter-node
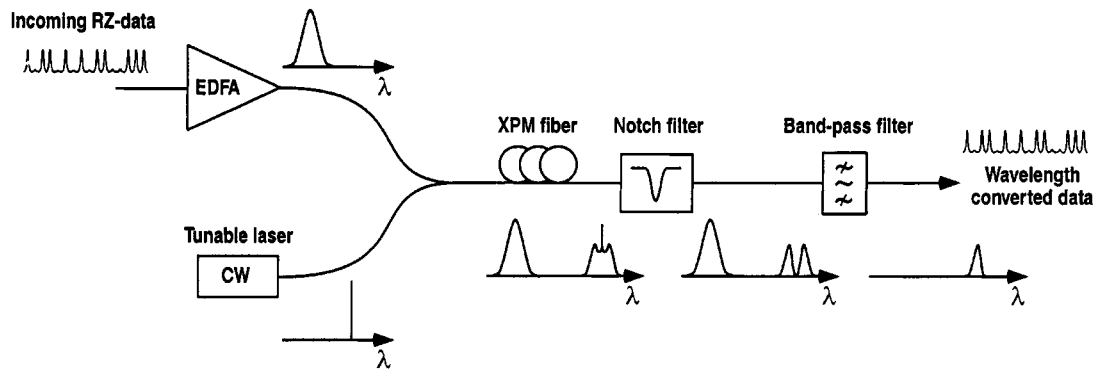
Fig. 8. Principle of operation of high-speed XPM fiber-based wavelength converter.
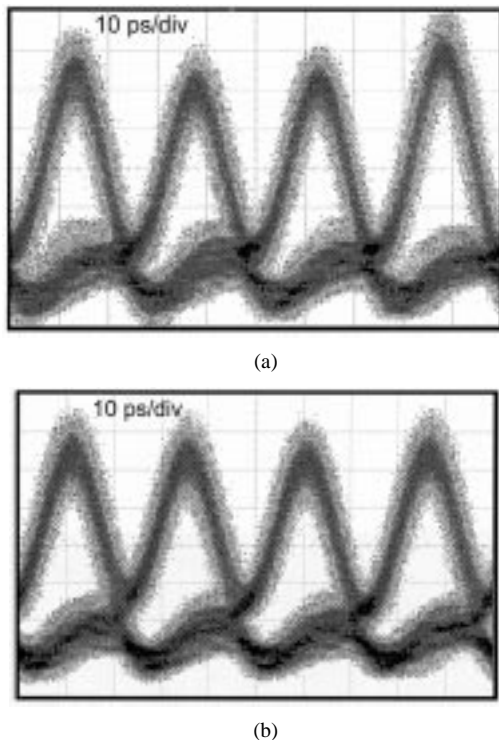

(a)

(b)

Fig. 9. (a) Nonlinear transmission characteristic of fiber XPM-WC and (b) 40 Gb/s original and converted eye diagrams.

distance and will help determine the required dynamic range of the burst-mode subcarrier receiver. Therefore, either dispersion compensation or dispersion insensitive detection techniques must be employed.

When the subcarrier signal is detected at a square law photoreceiver the subcarrier amplitude depends upon the phase difference between the two sidebands. When this signal is propagated through a fiber, the dispersion induces a relative time delay between the subcarrier sidebands. Thus the received power P_S has a dependence on the distance traversed in the fiber. For certain values of fiber length L (or ω_s for a fixed fiber length) the received power P_S is null and the signal is cancelled out. In a multihop system where the length of fiber through which the light travels is unknown, this effect will cause label loss.

By suppressing the subcarrier, the sidebands are detected as individual wavelengths carrying the same information and the beat products between each sideband and the optical carrier is no longer detected. Therefore, only the information modulated on the sidebands is recovered and dispersion induced fading is eliminated. We have successfully employed a fiber loop mirror (FLM) to solve the subcarrier fading problem while at the same time providing a means to simultaneously tap and erase SCM labels [14]. The fiber loop mirror, shown in Fig. 10(a), drops the suppressed carrier signals to the tap port for detection and label recovery. The pass-through port forward the baseband packet with erased label to a wavelength conversion stage. The filter peaks are designed with a period to match the ITU grid. The filter employs two birefringent elements of equal length oriented with principal axis at 45° to one another and a half wave plate with principal axes oriented at 45° with respect to the nearest birefringent element. The use of two birefringent elements of equal length in series produces a wide passband for transmission between the input port and the through port and a narrow passband for transmission between the input port and the OSCM extraction port. The filter can be implemented entirely in fiber using birefringent fiber and polarization controllers or it may be implemented using birefringent crystals. The transmission spectrum of an all-fiber version of the filter fabricated at UCSB is shown in Fig. 10(b) and was measured using a broadband light source and a high-resolution optical spectrum analyzer.

C. Wavelength Agile Sources

Packet wavelength conversion critically depends on the switching speed of a tunable laser used as the local source for the new wavelength. New multi-element widely tunable lasers with the capability of tuning over hundreds of channels represent the current state of the art in semiconductor laser development. There is a wide variety of tunable laser designs and they all have a number of common characteristics. They have active sections for gain integrated with passive waveguide elements that are used for wavelength control, they employ some form of grating architecture for wavelength discrimination, and all use carrier injection for tuning. In this paper we describe three of the most promising candidates to be used as wavelength agile sources—Sampled Grating DBR (SGDBR), Super Structure Grating DBR (SSGDBR) and Grating assisted co-directional Coupler with Sampled Reflector (GCSR). The second part of this section will describe recent advances in the fast switching of a GCSR laser.

1) Wavelength Agile Laser Structures: The Sampled Grating DBR (SGDBR) lasers were the first ones among the mentioned widely tunable laser structures [28]. The SGDBR
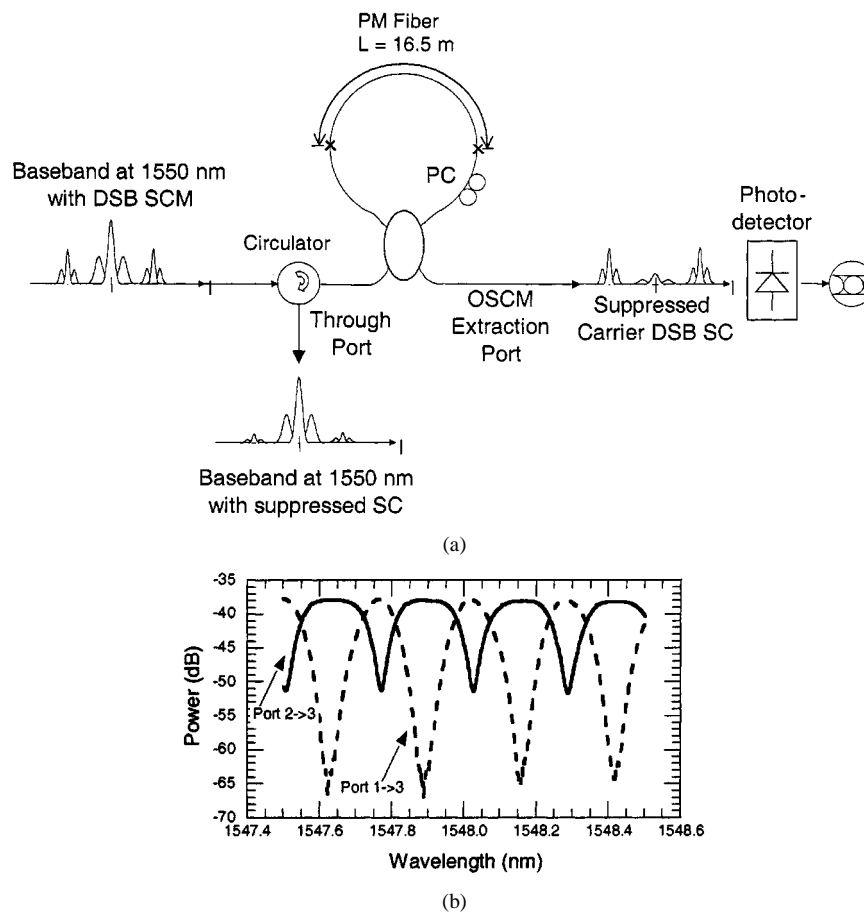
Fig. 10.   (a) Schematic of an all-fiber birefringent loop mirror filet (LMF). (b) Transmission spectrum of an all-fiber version of the filter.

is similar in structure to a DBR laser except that it employs a Vernier tuning mechanism to increase its tuning range. The SGDBR uses a pair of grating mirrors at either end of the cavity [Fig. 11(a)]. The gratings in the mirrors are periodically sampled which results in a sequence of equally spaced short grating bursts. These give the mirrors a comb like reflection spectrum with multiple equally spaced peaks. Different sampling periods are used in the front and back mirror to give them different peak spacing. This allows only a single pair of peaks to be aligned concurrently. The laser operates at the wavelength where the peaks from the front and back mirrors are aligned [Fig. 11(b)].

The Super Structure Grating DBR (SSGDBR) is a modification of the SGDBR design and is only different by the design of the mirrors [29], [30]. In the SSGDBR, the grating in the mirrors are periodically chirped instead of sampled. The advantage of this approach is that the grating occupies the entire length of the mirror so that a much higher reflectivity can be achieved with a lower coupling constant in the grating. The other main advantage is that the reflectivity of the individual peaks can be tailored such that all of the reflection peaks have the same magnitude.

The Grating assisted co-directional Coupler with Sampled Reflector (GCSR) [31], [32] device as the name indicated uses a grating assisted co-directional coupler within the laser as a frequency discriminator [Fig. 11(c)]. The wavelength selection is illustrated in Fig. 11(d). The coupler filter is tuned such that one peak of the comb generated by the Sampled

Reflector coincides with the maximum transmission of the coupler. The resulting reflectivity is a main peal surrounded by lower side peaks. The coarse tuning is obtained when only the coupler current is changed. The lasing wavelength is tuned in large steps corresponding to the reflector peak separation. Depending on the device the tuning range extends between 50 and 114 nm. The medium tuning occurs when both coupler and reflector are tuned at the same rate such as the same peak is selected all the time. The medium tuning range is between 5 and 15 nm, similar to the tuning range of a DBR laser. The fine tuning occurs when the phase current is changed. The lasing wavelength is tuned continuously over a cavity mode spacing. By combining the three types of tuning it is possible to obtain a truly continuous tuning, where any wavelength can be achieved.

2) Fast Switching Wavelength Agile Transmitters: By using proper driving circuitry and conditions it is possible to obtain fast (on the order of several nanoseconds) switching between ITU grid lasing modes over a broad range of wavelengths. We have demonstrated fast switching of the GCSR laser under digital control. Two arrays of HBT-based laser drivers were used to obtain different levels of output current that were used to drive coupler and reflector tuning sections, thus making it possible to achieve different lasing wavelengths. Schematic of this setup is shown in Fig. 12(a). If n laser drivers are used for both coupler and reflector sections, 2×2^n different channels may be accessed. Fig. 12(b) shows measured switching time for 36 chan-
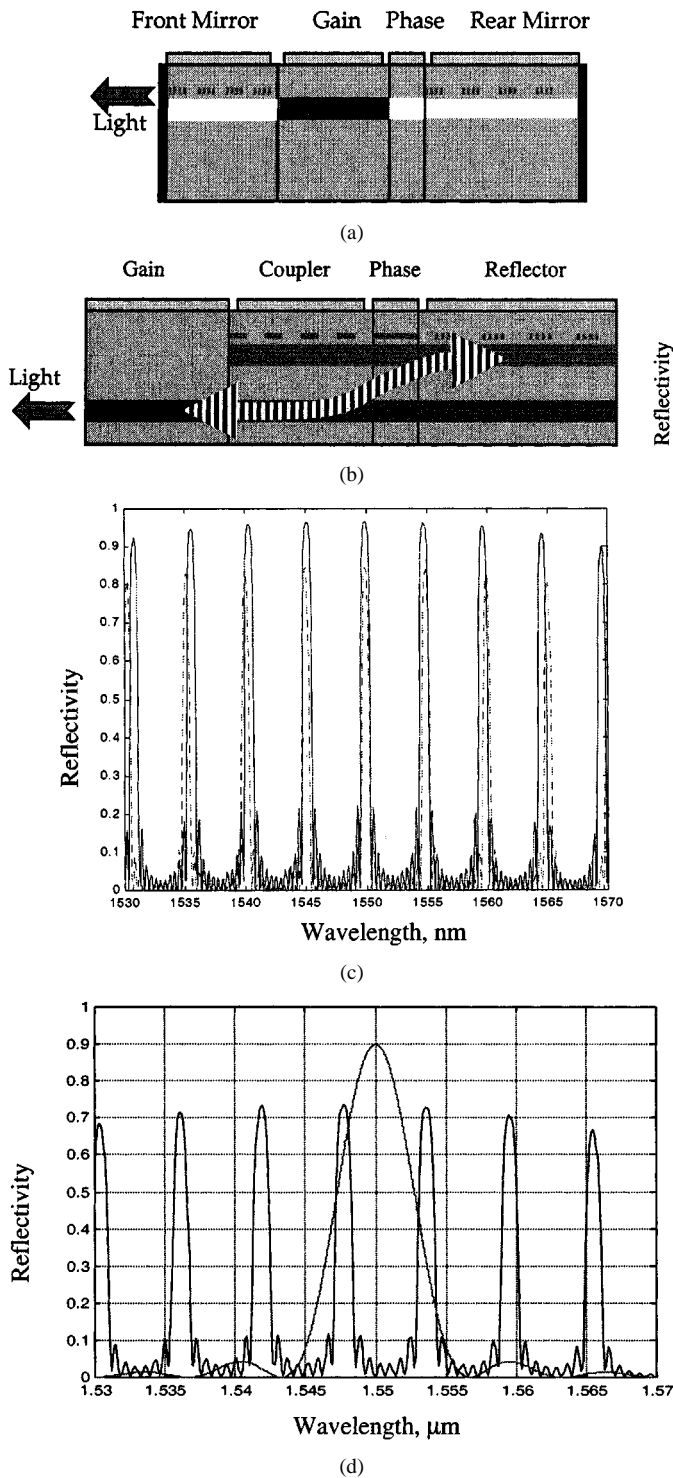
(a)

(b)

(c)

(d)

Fig. 11. SGDBR laser structure.

(a)

(b)

Fig. 12. (a) Schematic of fast switching using a GCSR laser and (b) measured switching times for 36 ITU frequency channels.

nels located on the ITU frequency grid. The longest switching time is less than 4.5 ns.

D. Electroabsorption Modulators for 40 Gb/s Packet Detection

High-speed demultiplexing is one of the key technology in high bit rate time-division-multiplexed transmission systems. Demultiplexing based on high-speed integrated circuit technology has been demonstrated at 60 Gb/s [33]; however, it has bee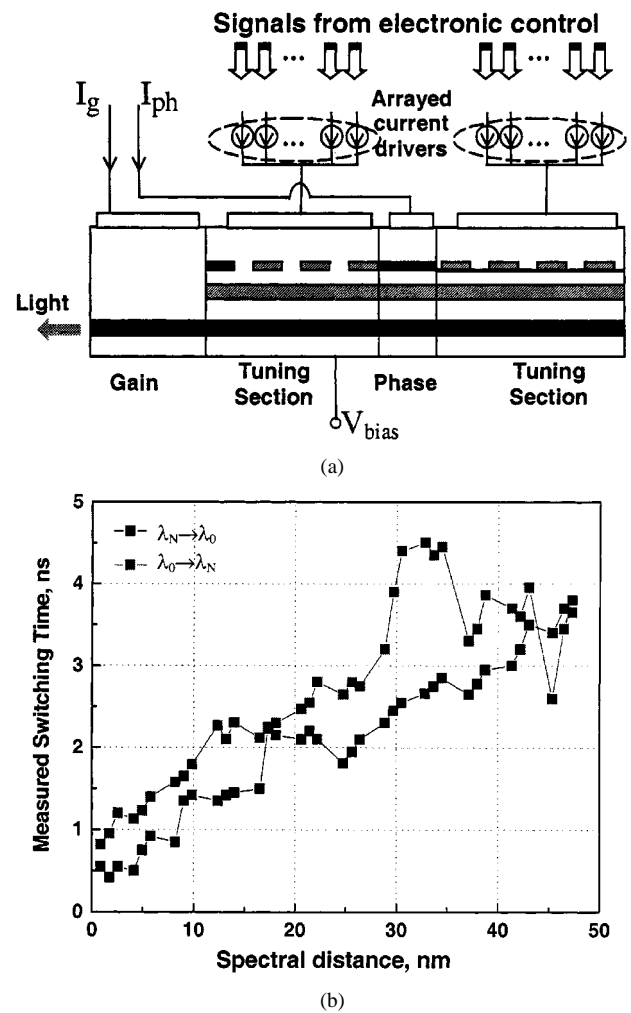n limited to 40 Gb/s in fiber transmission experiments. On the other hand, optical demultiplexing using a sinusoidally driven electroabsorption modulator (EAM) has emerged as a simple alternative approach to electrical demultiplexing [34], with demonstrations at bit rates up to 160 Gb/s [35]. Due to its nonlinear attenuation characteristic, a highly reverse biased EA modulator is capable of producing a short switching window with high extinction ratio for selecting the desired channel from the incoming data stream.

Optical demultiplexing based on EAMs fabricated at UCSB was recently deployed in the 40 Gb/s wavelength routing experiment [8]. The 400-μm long EA modulator is based on a traveling-wave electrode structure with ten periods of strain-compensated InGaAsP quantum wells fabricated by MOCVD on semi-insulating InP substrate [36], as shown in Fig. 13. The device achieved a maximum extinction of 38 dB while its modulation bandwidth was 16 GHz. The 400-mm EA modulator was reverse biased at -4.8 V and driven by a 6 V_{PP} 10 GHz RF signal to generate a 14-ps switching window, which was synchronized to the desired 40 Gb/s optical channel by an electrical delay line. The demultiplexed optical channel was then optically amplified and detected by a 10-GHz receiver.
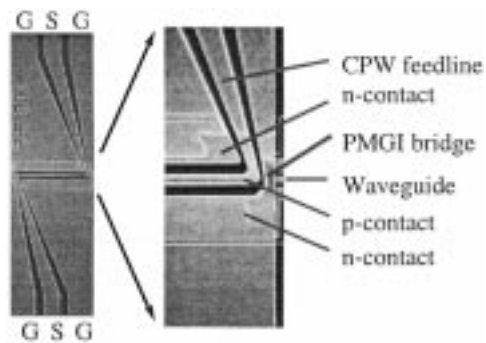
Fig. 13. High frequency EAM used for 40 Gb/s optical demultiplexing and (a) 40 Gb/s input and (b)–(e) demultiplexed outputs.
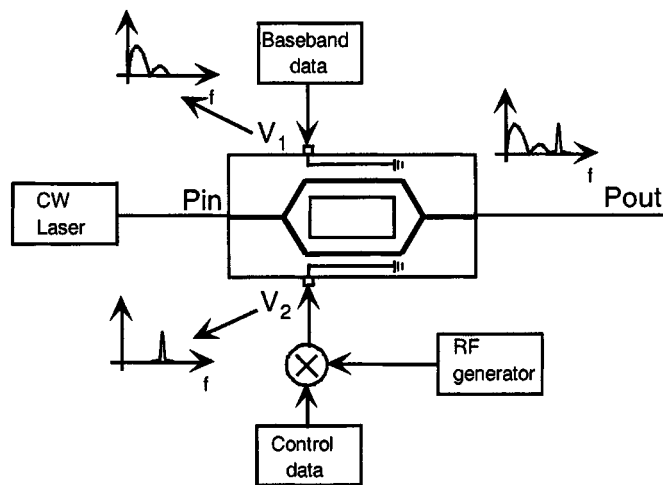

Fig. 14. Optical subcarrier multiplexed transmitter based on differential external modulator.

E. Packet Transmitters

Generation of packets requires compatible coding of the payload and label with the label swapping hardware within the network. In this section we describe transmitters that can generate packets with subcarrier or serial labels.

1) OSCM Transmitters: The ideal OSCM transmitter is one that is simple, robust, permits an arbitrary subcarrier to carrier modulation ratio, and does not introduce penalty into either the baseband data or the subcarrier signal. It is also desirable that the introduction of chirp in the baseband and subcarrier signals be avoided or controlled. In this section we describe two techniques for the generation of hybrid baseband and optically subcarrier multiplexed signals that have been employed at UCSB.

The first technique is the simplest to implement and most robust. In this technique a differential Mach–Zehnder external modulator is used to impress both the baseband data and the subcarrier signal onto the optical carrier simultaneously. Details of the tradeoffs for this type of transmitter are given in [11]. A schematic diagram of this transmitter is shown in Fig. 14. Only a single Mach–Zehnder modulator is employed to impress both the subcarrier signal as well as the baseband data onto the optical carrier. One port of the Mach–Zehnder is driven with the baseband signal and the other port receives the subcarrier signal. The second transmitter architecture that has been employed at

UCSB overcomes some of the disadvantages of the differentially driven Mach–Zehnder transmitter [14]. This design had, however, increased complexity and requires stability issues to be addressed. A schematic diagram of this transmitter is shown in Fig. 15(a). In this transmitter the baseband data and the subcarrier signal are impressed on the same optical carrier independently using two separate external modulators. The separate signals are then combined using an optical multiplexer. Because the signals are generated separately they can be optimized independently and their relative amplitudes controlled using optical attenuation prior to the multiplexer. In order to avoid coherent interference between the signals, filtering must be employed to remove the carrier from one of the signals. In addition, the subcarrier signal must be out-of-band relative to the baseband data signal or filtering of the baseband signal to remove spectral content of at the subcarrier frequency must be done. In our method both the multiplexing and the required filtering is achieved using a birefringent loop mirror filter shown in Fig. 15(b).

The principal advantage of this transmitter is that the strength of the subcarrier signal relative to the baseband signal may be easily controlled and that there is no subcarrier amplitude dependent penalty introduced in the baseband data. In addition, both the chirp of the subcarrier signal and the baseband data signal may be controlled independently. The primary disadvantage of this technique is that the filter spectral response must be stable relative to the laser wavelength necessitating tight temperature control of the birefringent elements in the filter or some type of closed loop locking arrangement.

2) Time Multiplexed Transmitters: For low bit rate transmitters, 10 Gb/s and below, the label and the payload will probably have the same data format and the whole packet can be encoded using conventional modulation techniques for either NRZ or RZ data format. For high bit rate transmitters, beyond 40 Gb/s, it will most likely be necessary to use OTDM transmitters where several low bit rate data streams are time multiplexed together. The label is attached to the packet, at a lower bit rate to allow lower cost label processing electronics to be used. Fig. 16 shows a possible implementation of such transmitter generating a 40 Gb/s IP-packet with a 2.5 Gb/s attached time domain label. The incoming low bit rate IP packet is demultiplexed and stored in an electronic $4 \times N$ memory bank that effectively acts as a serial to parallel converter. This memory bank can be made of fast electronic memory arranged in a way that it is possible fill the memory at the incoming bit rate and to read the four memory banks in parallel. Once the whole packet is stored, the four rows are read in parallel at 10 Gb/s. Since in practice electronic memory can not be read at 10 GHz, multiple memory banks operating at the speed of the memory have to be multiplexed together constituting a memory read at 10 GHz. Each 10 Gb/s electrical channel subsequently drives an optical RZ transmitter the gives 10 Gb/s RZ data with about 10 ps pulses, e.g., an integrated transmitter consisting of a DFB laser with two integrated EAMs. The relative timing between the 10 Gb/s channels are adjusted to be 25 ps between each channel by using optical delays. Finally the four channels are interleaved in a fiber coupler to generate a 40 Gb/s data sequence. The label is generated simply by encoding the label data at 2.5 Gb/s NRZ on light with the same wavelength as the RZ sources and then attached to the
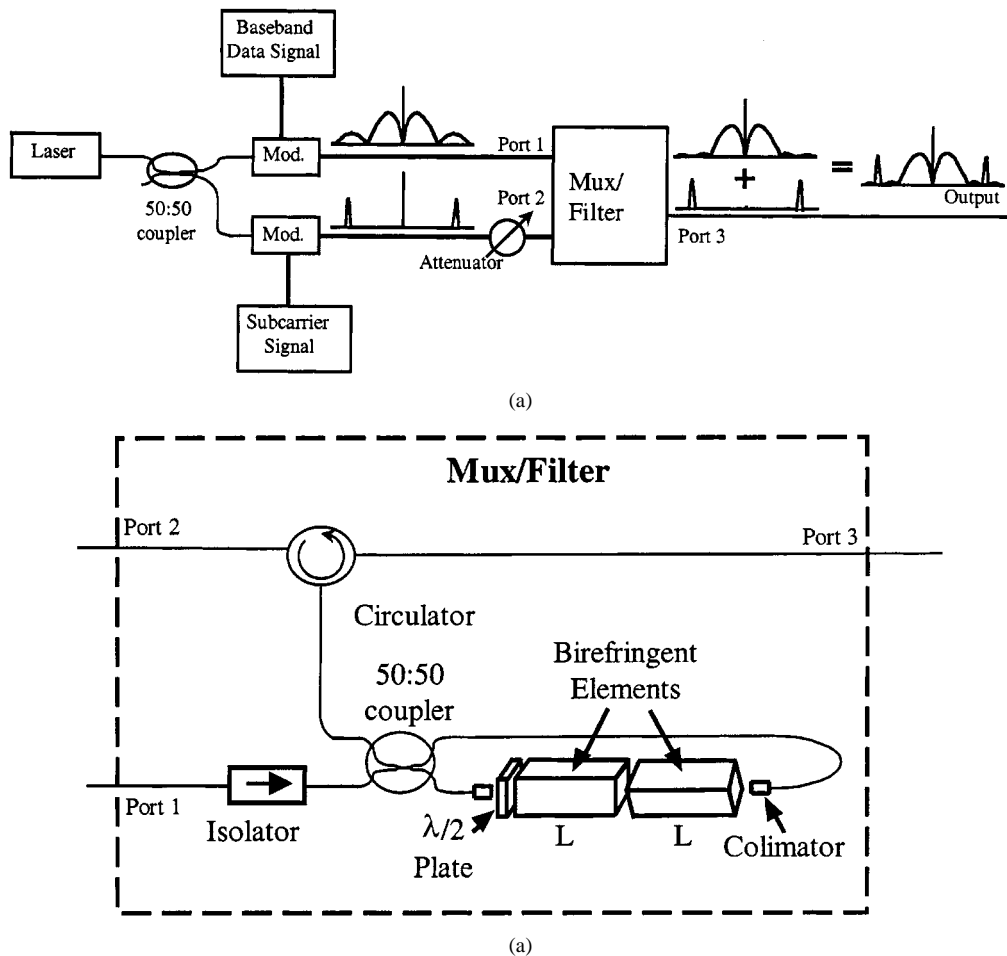
Fig. 15. Optically multiplexed SCM transmitter.
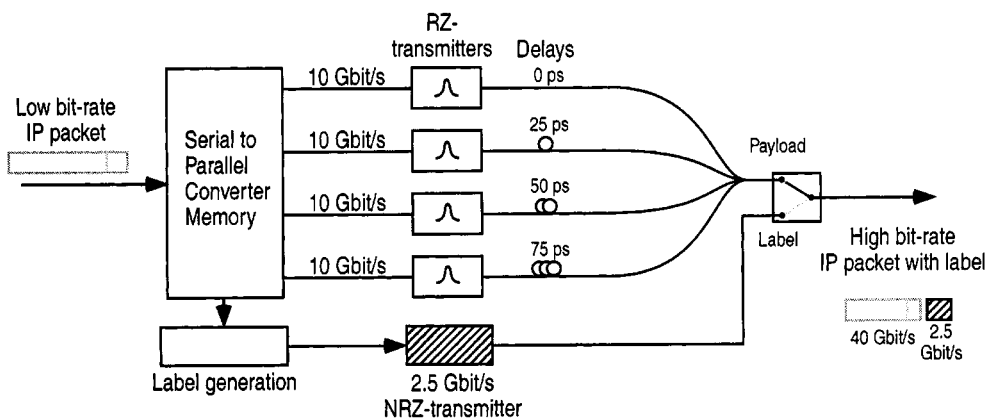
Fig. 16. Implementation of a high-speed packet serial label transmitter.

40 Gb/s packet after proper adjustment of the relative timing. Since all optical sources emit light at the same wavelength, it is in practice difficult to achieve the extinction ratio (ER) required from the sources when being in off-state. Therefore an optical switch is used at the output to avoid coherent crosstalk between the label source and the RZ data, This scheme can be extended to higher bit rates simply by increasing the number of rows in the serial to parallel converting memory and by decreasing the output pulse width from the RZ transmitters. The RZ transmitters can either be four individual transmitters con-stituted by DFB lasers with integrated electroabsorption modulators, or, if very short pulses are required, one common pulse source, e.g., a fiber ring laser, can be shared by four different data encoding modulators.

VII. AOLS SUBSYSTEM IMPLEMENTATIONS

In this section we review subsystems that realize the functions described in Fig. 4 using the technologies in the previous section.

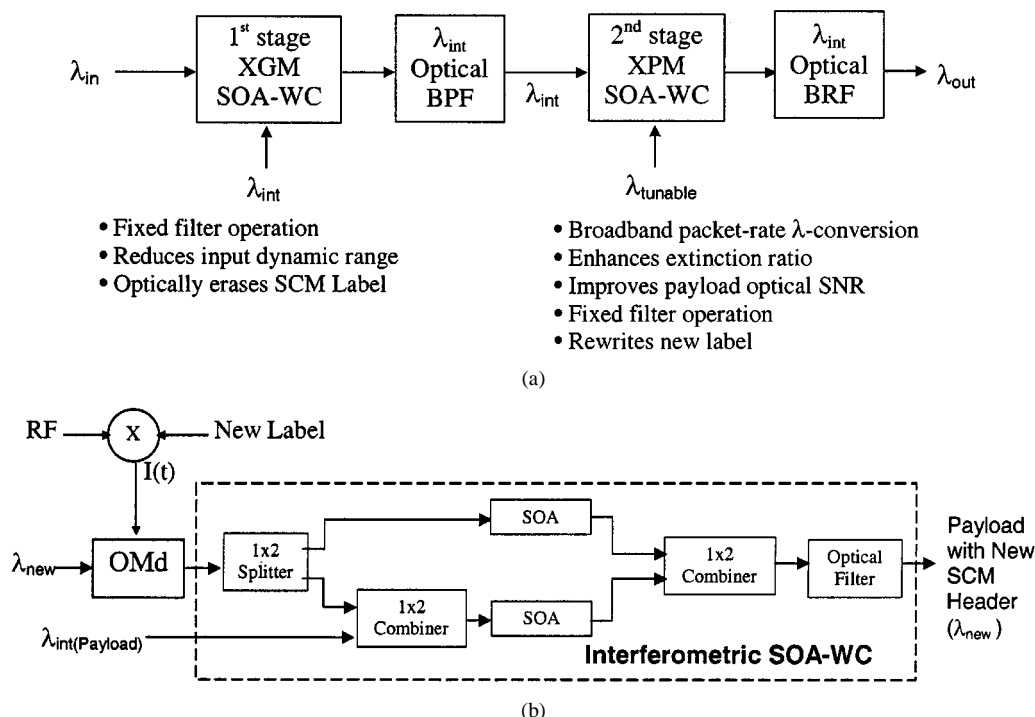Fig. 17. (a) Two-stage AOLS wavelength converter using cascaded SOA XGM and XPM modules and (b) second stage XPM-WC.

A. Two-Stage SOA Wavelength Converters with Subcarrier Labels

We have implemented and demonstrated an AOLS wavelength converter using a two-stage SOA wavelength converter module [37], [38] shown in Fig. 17(a). The two-stage geometry is designed to address key issues in wavelength conversion and optical label swapping. The XGM-WC stage erases the SCM header using the inherent low-pass filtering function of XGM wavelength conversion in SOAs, as described in [38]. It is also used to convert packets from an arbitrary network wavelength to a fixed internal wavelength allowing the use of fixed optical band pass filters (BPF) to pass only the internal wavelength and reject the original wavelength. Another key benefit of the two-stage geometry is that the first stage converts an arbitrary polarization at the input to a fixed polarization at the output for the second stage converter, making it easier to fabricate the XPM-WC technology. The first stage also reduces the packet optical power dynamic range and sets the packet average optical power level for the XPM-WC. The inverting operation of the XPM-WC is used in the second stage, as shown in Fig. 17(b) to provide noninverting operation after both stages. The highly nonlinear transfer function of the interferometric wavelength converter in the second stage is used to enhance the optical extinction ratio (2R regeneration) and convert the packet to an outgoing wavelength with a fixed band reject filter (BRF) that passes only the new tunable wavelengths. A fast wavelength tunable laser is utilized to enable packet-rate wavelength conversion. The new label is pre-modulated onto the fast tunable laser. As part of our NGI program we are leveraging recent developments in the field of photonic integrated circuits (PICs) to realize two-stage AOLS technology through integration of fast widely tunable lasers with SOAs, waveguides and on-chip wavelength monitors.

B. Fiber Loop Mirrors with Subcarrier Labels and Two-Stage SOA-WC

The fiber loop mirror (FLM) module provides label removal and a tap for SCM labels that is immune to fiber dispersion and utilizes a simple detector for label recovery. The packet without label is passed to the through port and may be injected into a two-stage AOLS-WC based on SOA technology as shown in Fig. 18. This architecture combines very high suppression of the original label over the complete ITU grid with the wavelength conversion and label rewriting properties of the integrated two-stage wavelength converters.

C. Fiber Wavelength Converters and Serial Labels

Optical label swapping of an attached time domain label to a packet can be implemented using the inherent nonlinear transfer function and differentiating nature of fiber XPM wavelength converter. The transmission function of the wavelength converter is highly nonlinear, which also depends on the derivative of the input signal. By using different data formats, bit rates, and power levels for the label and the payload, while keeping the energy per bit constant, it is possible to remove the label upon wavelength conversion.

A particular scheme that has been investigated is where the payload is in RZ format and the header is in NRZ format. This allows efficient use of bandwidth for the payload while retaining simplicity in handling the labels. If, for example, 10 ps pulses are used for a 40 Gb/s payload and 2.5 Gb/s NRZ data and if equal energy per received bit is assumed, the peak power of the labels will be 16 dB lower than the peak power of the payload. Thus the transmission through the wavelength converter will be extremely low. In addition the transmission through the wavelength converter depends on the derivative of the input
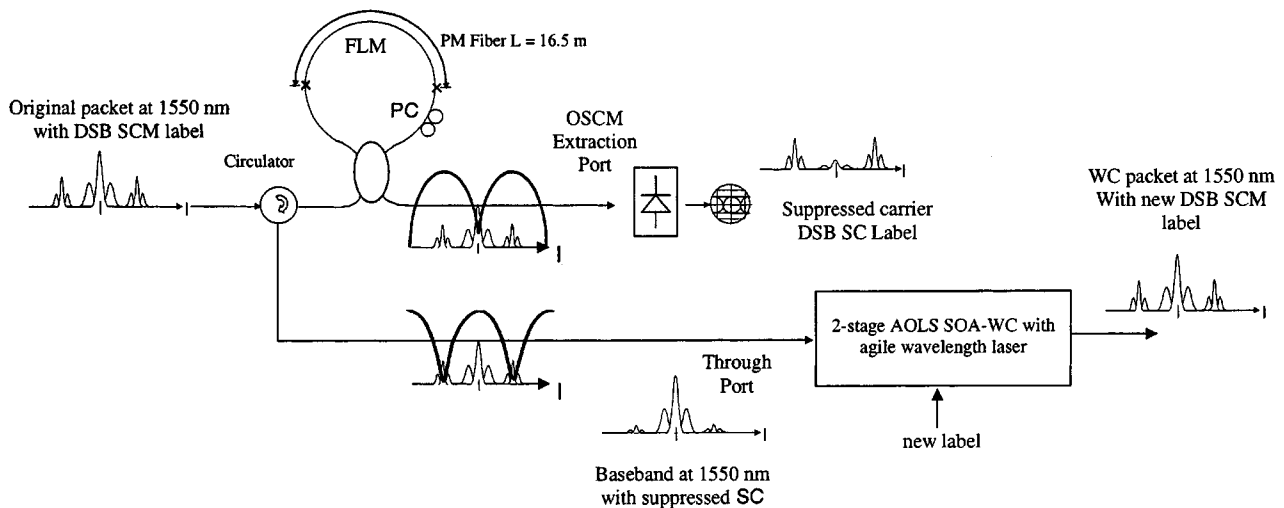
Fig. 18.   AOLS module using FLM to remove SCM label and two-stage AOLS-WC to convert packet and rewrite label.
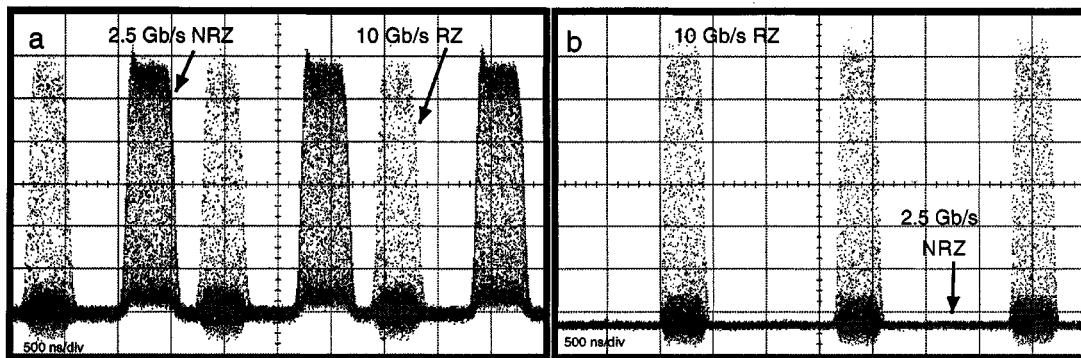

Fig. 19.   Packets of 2.5 Gb/s NRZ data and 10 Gb/s RZ data (a) before and (b) after wavelength conversion.

signal, why only transitions in the NRZ data will experience some transmission. All energy in the input data with zero derivative will be blocked in the wavelength converter, i.e. most energy in NRZ data will not drive the wavelength converter. After removing the incoming label a new label can easily be inserted either by adding a new label from a separate source after the wavelength converter or simply by premodulating the new label on the CW light that determines the output wavelength.

To demonstrate the concept of label replacement, a system similar to that in Fig. 8 was used. Packets of 10 Gb/s RZ data was mixed with 2.5 Gb/s NRZ as shown in Fig. 19(a). The frequency deviation that generates the optical side bands of the CW light will depend on the derivative of the input pulse power, which is turned into amplitude modulation after filtering. Due to this differentiating nature, the rise and fall times determine the conversion efficiency, which means that the wavelength converter will block low frequencies. In Fig. 19(b) it can clearly be seen how the 10 Gb/s RZ data is converted and the 2.5 Gb/s NRZ data is suppressed. It should be noted that NRZ data can not be converted, as only the edges of a signal are converted. In a sequence of consecutive ONEs, only the first ONE would generate an output signal. However, there would still be some output that could cause crosstalk when a new header is inserted, even though the old header data has been corrupted. For RZ data, the pulse width, and not the bit rate will determine the conversion ef-

ficiency. In another experiment, the 10 Gb/s RZ data and the 2.5 Gb/s NRZ data were switched manually, to measure the optical spectra, and to measure the penalty for rewriting new 2.5 Gb/s data where the original data was erased. At the input to the wavelength converter, the average power of the NRZ and the RZ data were equal and after removal of the original NRZ data a new 2.5 Gb/s NRZ data was inserted. The bit-error rate was measured for the original and rewritten data using $2^{31} - 1$ pseudo-random data and no penalty was observed due to the original data in the rewritten 2.5 Gb/s NRZ data. From the measurements it is clear that this type of wavelength converter can be used to passively erase a 2.5 Gb/s NRZ header from a high-speed RZ payload. Compared to other approaches using time-domain header [8], [39], no timing control is required to erase the header. New 2.5 Gb/s data can then be rewritten in different ways. Here a separate transmitter was used for the new data, which showed now crosstalk penalty from the previously erased data. This makes the system more stable compared to the approach of premodulating and slightly detuning the local CW light in the wavelength converter, but requires a high extinction ratio of the new header source when the payload is present. A third option, which has not been experimentally investigated, is to encode the new header by frequency modulating the local CW laser in the wavelength converter. With the present tuning speed of about 5 ns this would limit the bit rate to a maximum of 100 Mbit/s, but with
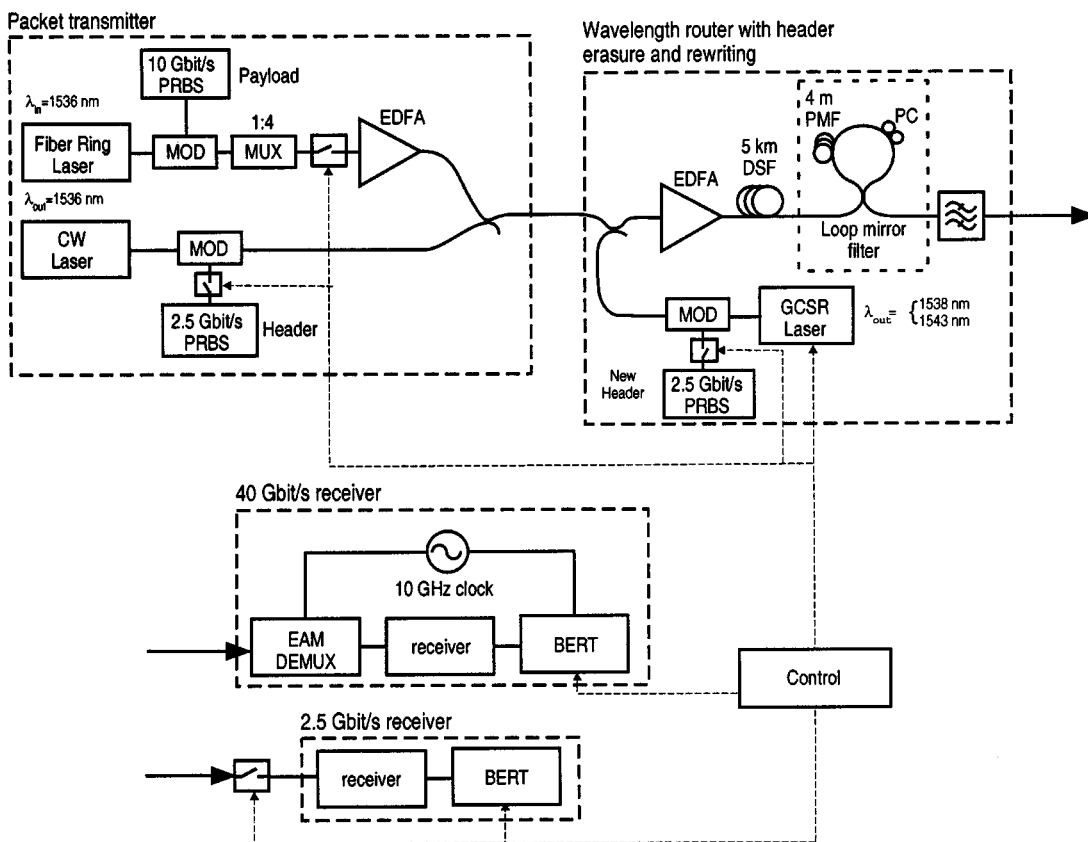
Fig. 20. Experimental setup of the packet routing experiment. MOD: LiNbO3 modulator; MUX: Passive 10–40 Gb/s multiplexer; EDFA: Erbium-doped fiber amplifier; DSF: Dispersion shifted fiber; PMF: Polarization-maintaining fiber; PC: Polarization controller; GCSR: Grating coupled sampled rear reflector laser; EAM DEMUX: Demultiplexer using an electro-absorption modulator; BERT: Bit-error-rate test set.

further advances in tunable laser technology this could be an interesting option.

VIII. EXPERIMENTAL DEMONSTRATIONS

A. 40 Gb/s AOLS Using Fiber XPM Wavelength Converter

To demonstrate AOLS at high bit rates an experiment was performed where packets of 40 Gb/s data was routed to different wavelengths using a wavelength converter. The 40 Gb/s payload was in RZ format and an attached time domain label was encoded using NRZ at 2.5 Gb/s. By using a fast tunable laser each packet can be routed to different wavelengths. The attached label is also replaced upon wavelength conversion by using the technique described in Section VII-C above.

Fig. 20 shows the experimental set-up. The packet generator consisted of an actively mode-locked fiber ring laser generating 10 ps at 1536 nm followed by a LiNbO3 modulator encoding 10 Gb/s data. The 10 Gb/s data were injected into a passive 10 to 40 Gb/s multiplexer and an acousto-optical modulator (AOM) gated out a 2.5 μs payload that was combined with a 2.5 Gb/s 500 ns long label. The label was aligned in front of the payload with 100 ns guard band determined by the 100 ns rise time in the AOM. A 100 ns guard band was inserted between each packet, giving a total packet length of 3.2 μs. The packets were then injected into the wavelength converter which consisted of an erbium-doped fiber amplifier (EDFA) followed by 5 km dispersion-shifted fiber (DSF) with a zero-dispersion wavelength
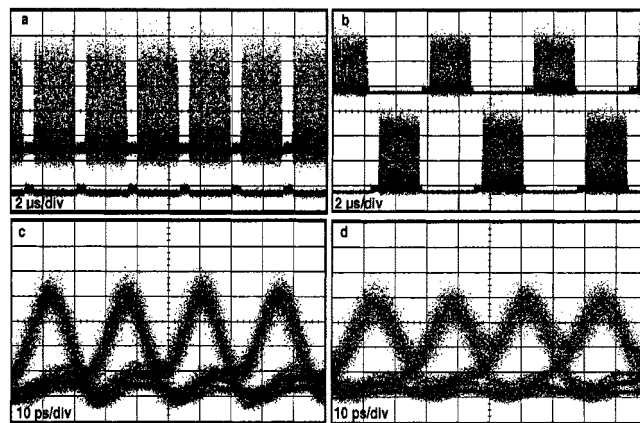
Fig. 21. (a) Packets and (c) 40 Gb/s eye-patterns before wavelength routing. (b) Packets routed to 1538 nm and 1543 nm and (d) eye pattern of routed packet at 1543 nm.

of 1542 nm. A fast tunable laser [31] that could be tuned to either 1538 or 1543 nm within 5 ns, determined the new wavelength. This laser was also used to encode the new 2.5 Gb/s label before entering the wavelength converter. After the DSF, a loop mirror filter was used to suppress the original CW light. A second filter was used to select one of the two sidebands and to suppress the original data. The use of only one sideband retained the pulse width and time bandwidth product (TBP) from the input pulse. The 40 Gb/s receiver consisted of a 40 Gb/s to 10 Gb/s demultiplexer followed by a 10 Gb/s preamplified

Fig. 22.   Subcarrier multiplexed AOL experiment with two-stage SOA-based label swapping and wavelength conversion.

receiver. The 2.5 Gb/s label receiver consisted of an AOM to remove the payload, which otherwise would dominate the measured optical average power, followed by an optically preamplified receiver. The BER measurements were made on both payload and label, and gat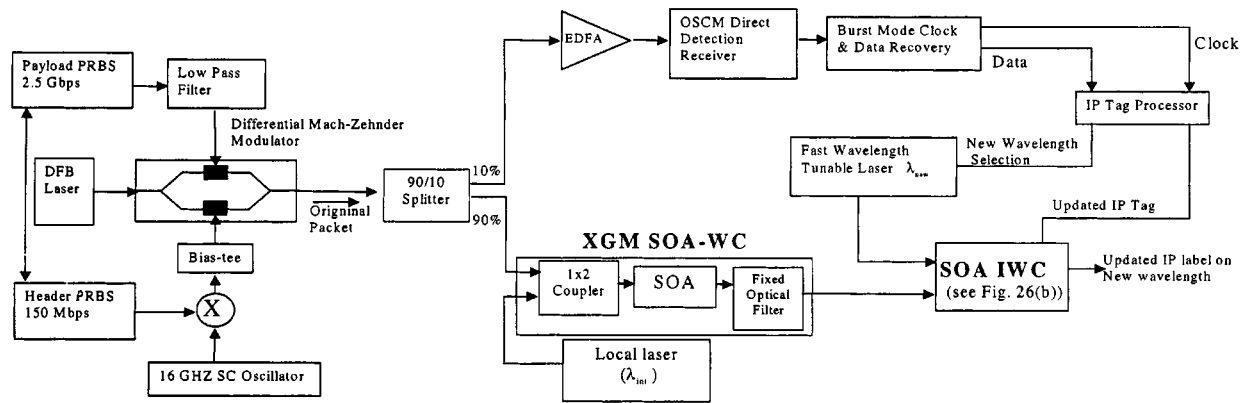ed to select appropriate time interval. Fig. 21(a) shows the input packets consisting of the 40 Gb/s RZ payload and the 2.5 Gb/s NRZ label with about 10 dB less peak power. In the lower trace the labels without the payload is reported. Fig. 21(b) shows every other packet routed to 1538 nm and 1543 nm with new inserted labels. The eye patterns shown in Fig. 21(c) and (d) was taken by zooming into the payload, before (1536 nm) and after wavelength converter (1543 nm). BER measurements were performed on both label and payload on incoming and outgoing packets and less than 4 dB penalty at a $BER = 10^{-9}$ was observed for all routed packets. The power penalty at a $BER = 10^{-9}$ for the replaced labels was less than 2.5 dB. For wavelength routing at 10 Gb/s, the penalty was less than 1 dB for the payload, which indicates that a major part of the penalty is due to instabilities in the 40 Gb/s data.

B. 2.5 Gb/s AOLS Using Two-Stage SOA Wavelength Converters

The WDM AOLS experiment that utilized a two–stage wavelength converter is shown in Fig. 22 [3], [4]. An OSCM packet transmitter was used to generate a 150 Mbps label on an RZ coded, ASK modulated 16 GHz subcarrier. Labels consist of a 16-bit preamble, an 84-bit tag and a 4-bit framing sequence. The payload is an NRZ coded, 2.5 Gb/s PRBS and the 16 GHz subcarrier supports payload bit rates out to 10 Gb/s. The packet duration is 1 ms. Label clock and data are recovered on a packet-by-packet basis following a 10% fiber tap, an EDFA and an OSCM direct-detection receiver. The OSCM receiver utilizes a fast Schottky barrier diode for envelope detection. A SAW filter is used to recover the tag clock for each packet and a fixed digital delay is needed to realign data and clock. A tag switching processor is required to perform serial-to-parallel conversion, compute a new label, multiplex the new label onto a RF subcarrier and set a fast wavelength tunable laser to the new wavelength within 12 ns.

A two-stage modified XGM/IWC was used to perform wavelength routing, optical label erasure and label rewriting at the IP packet rate. The OSCM label was removed during XGM due to the low pass frequency response of wavelength conversion in an SOA [38]. The XGM-WC converts incoming WDM packets to a fixed internal wavelength λ_{int} that is passed to the next stage using a fixed frequency optical filter. The XGM-WC is also used to set a stable operating point for the IWC. One arm of an InGaAsP IWC is injected with the optically filtered output of the XGM-WC. The output of a rapidly tunable 4-section GCSR laser transmitter is injected to both arms of the IWC. We measured the transmission BER for the label-switched payload with an observed maximum 4 dB power penalty for all four wavelengths. The power penalty is expected to decrease when optimally designed wavelength converters are used.

IX. SUMMARY

We have presented research results of the UCSB NGI project in AOLS. The AOLS approach to wire-rate packet encapsulation, routing and forwarding directly in the optical layer hold promise to support terabit-per-second fiber capacities independent of packet bit-rate and protocol. Two primary optical label coding techniques, serial- and subcarrier multiplexed-labels, were described and the functional blocks used to erase labels, rewrite labels, and convert packets to a new wavelength were reviewed. Issues involving burst-mode packet routing in an AOLS environment were discussed. Results were presented for both fiber and semiconductor-based technologies that have been used to perform AOLS functions. Key approaches to transmitting and processing subcarrier labels were described based on fiber loop mirrors used to realize supressed carrier, subcarrier label detectors that are immune to fiber dispersion induced signal fading. These taps can also be used to erase subcarrier labels in conjunction with semiconductor optical amplifer-based wavelength converters used to rewrite the labels and convert the packets to a new wavelength. Current work on highly integrated SOA-based AOLS modules was also described. For high bit-rates, new AOLS all-fiber wavelength converter subsystems were used to erase and rewrite 2.5 Gb/s serial encoded labels and wavelenth convert 40 Gb/s packets. We discussed how these technologies could be combined to realize AOLS subsystems. Key experimental system demonstration results were also presented.

ACKNOWLEDGMENT

REFERENCES

[1] A. Viswanathan, N. Feldman, Z. Wang, and R. Callon, "Evolution of multiprotocol label switching," *IEEE Commun. Mag.*, vol. 36, pp. 165–173, May 1998.

[2] A. Carena, M. D. Vaughn, R. Gaudino, M. Shell, and D. J. Blumenthal, "OPERA: An optical packet experimental routing architecture with label swapping capability," *J. Lightwave Technol.*, vol. 16, Dec. 1998. Special Issue on Photonic Packet Switching.

[3] D. J. Blumenthal, A. Carena, L. Rau, V. Curri, and S. Humphries, "All-optical label swapping with wavelength conversion for WDM-IP networks with subcarrier multiplexed addressing," *IEEE Photon. Technol. Lett.*, vol. 11, Nov. 1999.

[4] ——, "WDM optical IP tag switching with packet-rate wavelength conversion and subcarrier multiplexed addressing," presented at the Optical Fiber Communications/International Conference on Integrated Optics and Optical Fiber Communication'99, San Diego, CA, Feb. 21–26, 1999. Paper ThM1.

[5] D. Awduche, Y. Rekhter, J. Drake, and R. Coltun, "Multi-Protocol Lambda Switching: Combining MPLS Traffic Engineering Control with Optical Crossconnects,", 2001. Internet Draft, Work in Progress.

[6] P. Toliver, K.-L. Deng, I. Glesk, and P. R. Prucnal, "Simultaneous optical compression and decompression of 100-Gb/s OTDM packets using a single bidirectional optical delay line lattice," *IEEE Photon. Technol. Lett.*, vol. 11, pp. 1183–1185, Sept. 1999.

[7] C. Guillemot, M. Renaud, P. Gambini, C. Janz, I. Andonovic, R. Bauknecht, B. Bostica, M. Burzio, F. Callegati, M. Casoni, D. Chiaroni, F. Clerot, S. L. Danielsen, F. Dorgeuille, A. Dupas, A. Franzen, P. B. Hansen, D. K. Hunter, A. Kloch, R. Krahenbuhl, B. Lavigne, A. Le Corre, C. Raffaelli, M. Schilling, J.-C. Simon, and L. Zucchelli, "Transparent optical packet switching: The european ACTS KEOPS project approach," *J. Lightwave Technol.*, vol. 16, pp. 2117–2134, Dec. 1998.

[8] B. E. Olsson, P. Öhlén, L. Rau, G. Rossi, O. Jerphagnon, R. Doshi, D. S. Humphries, D. J. Blumenthal, V. Kaman, and J. E. Bowers, "Wavelength routing of 40 Gbit/s packets with 2.5 Gbit/s header erasure/rewriting sing all-fiber wavelength converter," *Electron. Lett.*, vol. 31, no. 4, pp. 345–347, Feb. 2000.

[9] P. Gambini, M. Renaud, C. Guillemot, F. Callegati, I. Andonovic, B. Bostica, D. Chiaroni, G. Corazza, S. L. Danielsen, P. Gravey, P. B. Hansen, M. Henry, C. Janz, A. Kloch, R. Krahenbuhl, C. Raffaelli, M. Schilling, A. Talneau, and L. Zucchelli, "Transparent optical packet switching: Network architecture and demonstrators in the KEOPS project," *IEEE J. Select. Areas Commun.*, vol. 16, pp. 1245–1259, Sept. 1998.

[10] A. Budman *et al.*, "Multigigabit optical packet switch for self-routing networks with subcarrier addressing," in *Optical Fiber Communications Conf. '92*, San Jose, CA, Feb. 4–7, 1992, pp. 90–91.

[11] D. J. Blumenthal, P. R. Prucnal, and J. R. Sauer, "Photonic packet switches: Architectures and experimental implementations," *Proc. IEEE*, vol. 82, no. 11, pp. 1650–1667, Nov. 1994. Invited Paper.

[12] R. Gaudino and D. J. Blumenthal, "A novel transmitter architecture for combined baseband data and subcarrier-multiplexed control links using differential Mach-Zehnder external modulators," *IEEE Photon. Technol. Lett.*, vol. 9, pp. 1397–1399, Oct. 1997.

[13] D. J. Blumenthal, J. Laskar, R. Gaudino, S. Han, M. Shell, and M. D. Vaughn, "Fiber optic links supporting baseband data and subcarrier-multiplexed control channels and the impact of MMIC photonic/microwave interfaces," *IEEE JLT/MTT Joint Special Issue on Microwave Photonics II, Trans. Microwave Theory Tech.*, vol. 45, pp. 1443–1452, Aug. 8, 1997.

[14] T. Dimmick, R. Doshi, R. Rajaduray, and D. Blumenthal, "Optically multiplexed transmitter for hybrid baseband and subcarrier multiplexed signals," presented at the Eur. Conf. Optical Communications'00, 2000.

[15] D. K. Hunter, M. C. Chia, and I. Andonovic, "Buffering in optical packet switches," *J. Lightwave Technol.*, vol. 16, pp. 2081–2094, Dec. 1998.

[16] Y. Ota and R. G. Swartz, "Burst mode compatible optical receiver with a large dynamic range," *J. Lightwave Technol.*, vol. 8, pp. 1897–1903, Dec. 1990.

[17] B. Sartorius, C. Bornholdt, O. Brox, H. J. Ehrke, D. Hoffmann, R. Ludwig, and M. Mohrle, "Bit-rate flexible all-optical clock recovery," presented at the Optical Fiber Communications Conference/International Conference on Integrated Optics and Optical Fiber Communication'99, San Diego, CA, Feb. 21–26, 1999. Paper FB1.

[18] D. Chiaroni, B. Lavigne, A. Jourdan, L. Hamon, C. Janz, and M. Renaud, "New 10 Gbit/s 3R NRZ optical regenerative interface based on semiconductor optical amplifiers for all-optical networks," in *Int. Conf. Integrated Optics and Optical Fiber Communication—Eur. Conf. Optical Communications'97*, vol. 5, Sept. 22–25, 1997, pp. 41–45.

[19] T. Durhuus, B. Mikkelsen, C. Joergensen, S. L. Danielsen, and K. E. Stubkjaer, "All-optical wavelength conversion by semiconductor optical amplifiers," *J. Lightwave Technol.*, vol. 14, pp. 942–954, June 1996.

[20] S. J. B. Yoo, "Wavelength conversion technologies for WDM network applications," *J. Lightwave Technol.*, vol. 14, pp. 955–966, June 1996.

[21] D. Wolfson and K. E. Stubkjaer, "Bit error rate assessment of 20 Gbit/s all-optical wavelength conversion for co- and counter-directional coupling scheme," *Electron. Lett.*, vol. 34, no. 23, pp. 2259–2261, Nov. 1998.

[22] C. D. Poole, R. W. Tkach, A. R. Chraplyvy, and D. A. Fishman, "Fading in lightwave systems due to polarization-mode dispersion," *IEEE Photon. Technol. Lett.*, vol. 3, pp. 68–70, Jan. 1991.

[23] B. E. Olsson, P. Öhlén, L. Rau, and D. J. Blumenthal, "A simple and robust 40 Gbit/s wavelength converter using fiber cross-phase modulation and optical filtering," *IEEE Photon. Technol. Lett.*, vol. 12, pp. 846–848, July 2000.

[24] B. E. Olsson and P. A. Andrekson, "Polarization independent all-optical AND-gate using randomly birefirngent fiber in a nonlinear optical loop mirror," in *Proc. Optical Fiber Comm. Conf.*, vol. 2, 1998, pp. 375–376.

[25] Y. Liang, J. W. Lou, J. K. Andersen, J. C. Stocker, O. Boyraz, M. N. Islam, and D. A. Nolan, "Polarization-insensitive nonlinear optical loop mirror demultiplexing with twisted fiber," *Opt. Lett.*, vol. 24, pp. 726–728, 1999.

[26] O. A. Lavrova, G. Rossi, and D. J. Blumenthal, "Rapid frequency tunable transmitter with large number of channels accessible in less than 5 ns," presented at the Eur. Conf. Optical Communications'00, 2000. Paper 6.3.5.

[27] P. V. Mamyshev, "All-optical data regeneration based on self-phase modulation effect," in *Eur. Conf. Optical Communications'98*, vol. 24, Madrid, Spain, 1998, pp. 475–476.

[28] B. Mason, S.-L. Lee, M. E. Heimbuch, and L. A. Coldren, "Directly modulated sampled grating DBR lasers for long-haul WDM communication systems," *IEEE Photon. Technol. Lett.*, vol. 9, pp. 377–379, Mar. 1997.

[29] H. Ishii, H. Tanobe, F. Kano, Y. Tohmori, Y. Kondo, and Y. Yoshikuni, "Broad-range wavelength coverage (62.4 nm) with superstructure-grating DBR laser," *Electron. Lett.*, vol. 32, no. 5, pp. 454–455, Feb. 1996.

[30] M. Öberg, P.-J. Rigole, S. Nilsson, T. Klinga, L. Backbom, K. Streubel, J. Wallin, and T. Kjellberg, "Complete single mode coverage over 40 nm with a super structure grating DBR laser," *J. Lightwave Technol.*, vol. 13, pp. 1892–1898, Oct. 1995.

[31] M. Öberg, S. Nilsson, K. Streubel, J. Wallin, L. Backbom, and T. Klinga, "74 nm wavelength tuning range of an InGaAsP/InP vertical grating assisted codirectional coupler laser with rear sampled grating reflector," *IEEE Photon. Technol. Lett.*, vol. 5, pp. 735–738, July 1993.

[32] P.-J. Rigole, S. Nilsson, L. Backbom, T. Klinga, J. Wallin, B. Stalnacke, E. Berglind, and B. Stoltz, "114-nm wavelength tuning range of a vertical grating assisted codirectional coupler laser with a super structure grating distributed bragg reflector," *IEEE Photon. Technol. Lett.*, vol. 7, pp. 697–699, July 1995.

[33] A. Felder, M. Moller, M. Wurzer, M. Rest, T. F. Meister, and H.-M. Rein, "60 Gbit/s regenerating demultiplexer in SiGe bipolar technology," *Electron. Lett.*, vol. 33, pp. 1984–1986, 1997.

[34] M. Suzuki, H. Tanaka, and Y. Matsushima, "10 Gbit/s optical demultiplexing and switching by sinusoidally driven InGaAsP electroabsorption modulators," *Electron. Lett.*, vol. 28, pp. 934–935, 1992.

[35] B. Mikkelsen, G. Raybon, R. J. Essiambre, K. Dreyer, Y. Su, L. E. Nelson, J. E. Johnson, G. Shtengel, A. Bond, D. G. Moodie, and A. D. Ellis, "160 Gbit/s single-channel transmission over 300 km nonzero-dispersion fiber with semiconductor based transmitter and demultiplexer," presented at the ECOC'99, vol. PD2-3, 1999.

[36] S. Z. Zhang, Y. J. Chiu, P. Abraham, and J. E. Bowers, "25 GHz polarization-insensitive electroabsorption modulators with traveling-wave electrodes," *IEEE Photon. Technol. Lett.*, vol. 11, pp. 191–193, 1999.

[37] B. Mason, G. Fish, and D. J. Blumenthal, Integrated wavelength tunable single and two-stage wavelength converter.

[38] M. D. Vaughn and D. J. Blumenthal, "All-optical updating of subcarrier encoded packet headers with simultaneous wavelength conversion of baseband payload in semiconductor optical amplifiers," *IEEE Photon. Technol. Lett.*, vol. 9, pp. 827–829, June 1997.

[39] P. Öhlén, B. E. Olsson, and D. J. Blumenthal, "All-optical header erasure and penalty-free rewriting in a fiber-based high-speed wavelength converter," *IEEE Photon. Technol. Lett.*, vol. 12, pp. 663–665, 2000.

Timothy E. Dimmick received the B.S. degree in electrical engineering from the University of Maryland, College Park, in 1983 and the Ph.D. degree (also from the University of Maryland) in 1990.

He is a visitor to the Optical Communications and Photonic Networks (OCPNs) from the Laboratory for Physical Sciences, College Park, MD. His research work includes the development of all fiber narrow-band acoustooptic tunable filters, fiber-optic sensors, optically preamplified receievers, ultrafast diode-pumped solid-state lasers, and coherent light detection and optical signal processing systems. He is currently working to develop optical network performance monitoring techniques using optical subcarrier multiplexed signals.

Daniel J. Blumenthal (S'91–M'93–SM'97) received the B.S.E.E. degree from the University of Rochester, NY, in 1981, the M.S.E.E. degree from Columbia University, NY, in 1988, and the Ph.D. degree from the University of Colorado, Boulder, in 1993.

From 1993 to 1997, he was Assistant Professor in the School of Electrical and Computer Engineering at the Georgia Institute of Technology. He is currently the Associate Director for the Center on Multidisciplinary Optical Switching Technology (MOST) and Associate Professor in the Department of Electrical and Computer Engineering at the University of California, Santa Barbara. He heads the Optical Communications and Photonic Networks (OCPNs) Research. His current research areas are in optical communications, wavelength division multiplexing, photonic packet switched and all-optical networks, all-optical wavelength conversion, optical subcarrier multiplexing, and multispectral optical information processing.

Dr. Blumenthal is recipient of a 1999 Presidential Early Career Award for Scientists and Engineers (PECASE) from the White House and the DoD, a 1994 NSF Young Investigator (NYI) Award and a 1997 Office of Naval Research Young Investigator Program (YIP) Award. He is a member of the Optical Society of America (OSA) and the IEEE Lasers and Electro-Optics Society (LEOS).

Lavanya Rau received the Masters degree in physics in August 1995 from the Indian Institute of Technology, Bombay. She is currently pursuing the Ph.D. degree in optical communication at the University of California, Santa Barbara.

She worked at the Lawrence Livermore National Laboratory in the summer of 1997, where she studied the effectiveness of AOTF in the NTONC Network. Her research interests include optical wavelength conversion, optical subcarrier multiplexing, and optical internet protocol routing.

Milan Mašanović was born in Pancevo, Yugoslavia, on August 7, 1974. He graduated from the School of Electrical Engineering, University of Belgrade, Yugoslavia, in 1998. He received the M.Sc. degree in electronics and photonics in 2000. and is currently working on the Ph.D. degree in Electrical and Computer Engineering Department, University of California at Santa Barbara.

His current research includes design of photonic integrated circuits and their applications in optical label swapping architectures.

Bengt-Erik Olsson received the Ph.D. degree in May 1998 from Chalmers University of Technology, Sweden, where he worked on applications of the nonlinear optical loop mirror as well as development of measurement technologies for polarization mode dispersion.

After receiving the Ph.D. degree, he worked within the European ACTS program MIDAS on two field experiments deploying solitons and midspan spectral inversion at 40 Gb/s and 80 Gb/s transmission. In January 1999, he joined Prof. Blumenthal's group at the University of California at Santa Barbara (UCSB) working on high-speed optical networking issues. He has authored or coauthored over 30 technical papers within these research activities.

Olga Lavrova (S'00) was born in St. Petersburg, Russia, in 1974. She received the B.S. degree in physics and the M.S. degree in electrical engineering from the St. Petersburg State Electrical Engineering University. In 1997, she joined the Electrical and Computer Engineering Department of the University of California at Santa Barbara and is currently pursuing the Ph.D. degree in the Optical Communications and Photonic Networks Laboratory.

Her current work includes experimental and analytical studies of widely tunable semiconductor lasers and their applications in optical network systems.

Giammarco Rossi received the "laurea" degree in electronic engineering with honors from the University of Pavia, Italy, in 1994 with a thesis on quantum effects in photodetection. As a Ph.D. student, he worked in the Optoelectronics device research unit of CSELT (Centro Studi E Laboratori Telecomunicazioni, Torino, Italy) and in the Optoelectronic research group of the University of Pavia. He received the Ph.D. degree in electronics in 1999 from the University of Pavia with a dissertation on high-speed semiconductor lasers for advanced optical communication systems.

Dr. Rossi is the recipient of the best thesis in optoelectronics of the year 1999 by the LEOS Italian chapter.

Roopesh Doshi received the B.S. degree in electrical engineering from the California Institute of Technology, Pasadena, in 1998. He is currently working towards the Ph.D. degree in the Electrical and Computer Engineering Department of the University of California at Santa Barbara.

He joined AstroTerra Corporation, San Diego, CA, where he worked on a wide area testbed for a free-space laser communications network, as well as a ship-to-shore free-space laser communications system. His research areas are performance monitoring, all-optical label swapping, and optical internet protocol routing.

Olivier Jerphagnon received the Masters degree in electrical and computer engineering from the Grenoble Institute of Technology (INPG), France, in July 1998. He then continued his academics at the University of California at Santa Barbara (UCSB) as a Teaching Assistant in the Electrical and Computer Engineering Department, and as part of the Optical Communication and Photonics Networks research group. He received the Master of Science degree in electronics and photonics from UCSB in December 1999.

His research interests include high-frequency electronics, fiber optics communication, and new generation of optical networks. He is now an Optical Engineer at Calient Networks.

John E. Bowers (S'78–M'81–SM'85–F'93) received the M.S. and Ph.D. degrees in applied physics from Stanford University, Stanford, CA.

He is CTO and cofounder of Calient Networks. He is on leave from University of California at Santa Barbara (UCSB), where he is director of the Multidisciplinary Optical Switching Technology Center (MOST), and a professor in the Department of Electrical Engineering at the University of California, Santa Barbara. He has worked for AT&T Bell Laboratories and Honeywell before joining UCSB. He has published five book chapters, over 300 journal papers, over 300 conference papers and has received 18 patents.

Dr. Bowers is a Fellow of the American Physical Society, a recipient of the IEEE LEOS William Streifer Award, Sigma Xi's Thomas F. Andrew prize, and the NSF Presidential Young Investigator Award.

Volkan Kaman received the B.S. degree in electrical engineering from Cornell University, Ithaca, NY, in 1995, the M.S. degree from the University of California at Santa Barbara (UCSB) in 1997, and the Ph.D. degree from UCSB

His research interests are in high-speed electrical and optical TDM systems and applications of electroabsorption modulators for optical processing.

Larry A. Coldren (S'67–M'72–SM'77–F'82) received the Ph.D. degree in electrical engineering from Stanford University, Stanford, CA, in 1972.

After 13 years in the research area at Bell Laboratories, he was appointed Professor of Electrical and Computer Engineering at the University of California at Santa Barbara (UCSB) in 1984. In 1986, he assumed a joint appointment with Materials and ECE. At UCSB, his efforts have included work on novel guided-wave and vertical-cavity modulators and lasers as well as the underlying materials growth and dry-etching technology. He is now investigating the integration of various optoelectronic devices, including optical amplifiers and switches, tunable lasers, receivers, and surface-emitting lasers. He is also heavily involved in new materials growth and fabrication technology essential to the fabrication of such integrated optoelectronic components. He has authored or coauthored over 300 papers, three book chapters, and one textbook, and has been issued 26 patents.

He is a Fellow of the Optical Society of America (OSA), a past Vice-President of IEEE-LEOS, and has been active in technical meetings. He is currently Director of the multicampus DARPA supported Heterogeneous Optoelectronic Technology Center.

John Barton, photograph and biography not available at the time of publication.